Analysis of Overmoded Waveguides Using the Finite-Difference Time Domain Method

D. H. Roper, J. M. Baird

Microwave Device and Physical Electronics Laboratory
Department of Electrical Engineering
University of Utah, Salt Lake City, 84112

Abstract

This paper presents techniques developed for analyzing scattering and coupling in overmoded waveguides using the Finite-Difference Time Domain method. Sources and absorbing boundary conditions for waveguide modes are examined. The stair-step approximation to round surfaces is considered, and a technique is described for finding the effective radius of a cylindrical model. A numerical example of scattering from a step diameter transition in circular waveguides is presented and compared to the analytic solution.

I. Introduction

The computational efficiency of the Finite-Difference Time Domain (FDTD) technique has made it the method of choice for analysis of electrically large objects. The FDTD method has been used with dominant-mode rectangular waveguides to analyze aperture coupling [1] and to excite cavities. [2,3] However, the use of this technique for mode scatter analysis in overmoded waveguides has not been observed in the literature. In this paper we use the Induction Theorem to create total field zones and scattered field zones in problems involving overmoded rectangular and circular waveguides for High Power Microwaves. This represents a new technique for analyzing scattered modes in oversized waveguides. The FDTD formalism is by now well known [4] and will not be presented here.

Using equivalent surface currents on the excitation planes, it is relatively easy to launch any desired mode or combination of modes in the total field region of a waveguide model. This method reduces sensitivity to unwanted reflections from absorbing boundaries, and allows for reduced model sizes and/or increased mesh resolutions. High-frequency transients and stair-step approximations to cylinders are important problems which must be addressed in order to obtain accurate results. The standard free space absorbing boundary conditions perform very poorly as waveguide terminations, but simpler equations can be used successfully. These work best with single-mode excitations but their performance deteriorates when many modes exist. As a numerical example, mode scatter from a step transition in circular waveguides was calculated and the results agreed closely with the analytic solution.

II. Source Conditions

Desired characteristics of an FDTD source condition are the ability to launch any mode at a selected amplitude, and an excitation plane that is 'transparent' to scattered/reflected fields. The latter condition is needed to avoid artificial reflections from the source plane, which produce a cavity effect and can cause the simulation to be unstable, i.e. the field magnitudes grow in time and do not converge to steady state values.

As stated, an FDTD version of the Electromagnetic Induction Theorem [5] has been implemented to launch specific modes in a waveguide model. Equivalent surface currents are used at a fixed frequency to separate the FDTD lattice into regions containing total fields and scattered fields only, as shown in Figure 1. A Total Field Zone (TFZ) is created between two transverse planes where selected waveguide scatterers can be modeled. With no scatterer inside, the fields outside the TFZ should be zero. The incident fields are added in at the source planes (boundaries of the TFZ) by means of current terms in Maxwell's Equations, allowing the scattered fields to pass through. Multiple mode patterns can be excited by calculating the surface currents for each mode individually and applying them in this way. The scattered modes can pass out of the TFZ and be recorded in the scattered field regions on either end with greater dynamic range. Absorbing boundaries, or Radiation Boundary Conditions (RBC's), are the terminations.

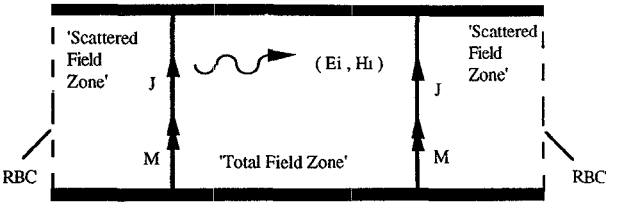

Figure 1 Induction Equivalent model used to launch modes in a waveguide .

Previously, the lattice zoning technique has been used by others to calculate the bistatic RCS of 3D objects. [4,6] A few modifications are required to make it work in waveguides. The application of this technique is anticipated in Reference [2], but to our knowledge this is the first time that the technique has been used to create a Total Field Zone in waveguides or to launch higher-order modes.

Because the fields outside the TFZ are usually small, very little energy is reflected back by the RBC's. What is reflected will propagate through the model and be mostly absorbed again by the RBC's on the other end, so sensitivity to unwanted reflections at the absorbing boundaries is greatly reduced. Therefore, the source planes can be made very close to the boundaries to provide better computational efficiency.

CH3141-9/92/0000-0401$01.00 © 1992 IEEE

Figure 2 shows the simulation of a TM_{01} mode in a circular waveguide with a coaxial probe. The short dashes which are plotted at each mesh point represent the magnitude and direction of the electric field vectors. This plot clearly shows the two planes which define the Total Field Zone. The model was used to calculate coupling to and scatter from the probe and the results agreed well with measured data. [10]

Figure 3 shows time history data for points inside and outside the TFZ in a uniform section of waveguide. The time history plots are for E_x at identical positions in the transverse plane but at different z coordinates. The results indicate that the useful dynamic range in finding scattered modes by this technique will probably extend to field ratios up to 100:1. This is based on the observed ratio of the fields in the total and scattered field regions. This ratio is not quite as good as values obtained in free space simulations such as RCS calculations, but it is still sufficient for many waveguide applications.

III. Initial Conditions

An important numerical consideration is the initial turn-on of the source. The fields are effectively multiplied by a step function u(t) which causes higher harmonics to be excited. These high-frequency transients die out slowly because of the dispersive properties of the rectangular mesh [4], so a very long run time would be needed to reach steady state. This problem is more serious in waveguides than it is in free space problems because of the closed resonant structure. The choice of a cosine or a sine excitation is immaterial here. The function $u(t)\cos(\omega t)$ obviously produces a step at t=0 for the transverse fields. The function $u(t)\sin(\omega t)$ has a step in derivative, so the z-directed fields (which are not sourced) are discontinuous.

The solution that has been used is to apply a ramp envelope to the fields at the start of the simulation. Linear and exponential ramp functions were tried with no observable improvement, but a raised cosine function, given by equation (1), has been used with good success. This has the desirable properties that both the function and its first derivative start at zero and are continuous. The ramp is programmed to rise up over 2-3 cycles of the source frequency, and this is sufficient to reach steady state in a reasonable time.

$$f(t) = \begin{cases} 0 & t < 0 \\ 0.5[1-\cos(\omega_r t)] & 0 \le t \le \frac{T_r}{2} \\ 1 & t > \frac{T_r}{2} \end{cases} \qquad (1)$$

where T_r is the period of the ramped cosine (~3 source cycles).

IV. Modeling the Cylinder

For circular waveguides an FDTD code based on cylindrical coordinates would be preferred. However, when other objects such as sidewall probes are included in the model, we must return to a rectangular mesh. It is well known that the stair-step approximation can shift the resonant frequency of circular objects by several percent. [4] This problem is illustrated by figure 4, which shows initial time history data from a point in the scattered field region for a uniform waveguide. The fields at this point do not decay to zero as expected. The problem is due to an error in the assumed phase velocity, preventing the mode from being properly cancelled on one source plane.

The effective radius of the cylinder can be found by making a short TM_{010} cavity from a section of the cylinder and determining the resonant frequency. The fields are preloaded at the start of the simulation and left to oscillate naturally. The initial conditions

$$E_z(\rho,\phi,z) = J_0\left(\chi_{01}\frac{\rho}{a}\right) \qquad \mathbf{H} = 0 \qquad (2)$$

satisfy Maxwell's Equations for the cavity, and the fields converge to steady state very quickly. For the particular geometry described by figure 4, the oscillation frequency was found from time history data to be 98.9% of the expected value. The cell size was then adjusted to obtain the correct diameter and the improved result of figure 3(b) was obtained using a cylinder with 29 cells inside diameter. This procedure can allow accurate predictions to be obtained with less spatial resolution needed to model the cylinder, reducing computer memory requirements.

V. Radiation Boundary Conditions

Absorbing boundaries or Radiation Boundary Conditions (RBC's) are used to terminate the waveguide model. The standard free space conditions (Mur 2nd Order [7]) perform very poorly in this application, producing large reflections which make the simulated waveguide fields unstable. This is probably due to discontinuous field derivatives at the walls, which are difficult to account for in a stepped cylinder.

Three other types of RBC's were examined. The most successful method tested was the Mur 1st Order RBC, which can be used to customize the boundary for the excited mode. The second RBC investigated is a TEM type boundary condition. [8] This technique has successfully been applied to other transmission line models, and it also gave better results than the free space equations. Finally, a one-dimensional version of Mur 2nd Order was investigated. This method caused the fields to diverge more slowly than the standard Mur 2nd Order, but the simulated fields were still unstable. Of the three methods tested, the Mur 1st Order RBC gave superior results. This works very well for single-mode excitations, but gets worse when many modes are present, as will be shown in section VI. A good RBC for multiple modes must still be developed.

VI. Numerical Example

We now apply the FDTD method to calculate the transmission and reflection of a step diameter transition in circular waveguides. Waveguide I has a 0.764" radius and waveguide II has a 1.0" radius. These values were determined by the method of section IV. The frequency of operation is 11.0 GHz, and the RBC's in each waveguide were optimized for the TE_{11} mode.

The exact solution was determined by expressing the transverse fields in terms of expansions over the basis field vectors in each waveguide. [5,9] Matching the transverse fields at the junction using truncated infinite series leads to the overall voltage scattering matrix of the step. The intermode coupling coefficients were determined by dot multiplying the basis vectors and integrating over the common area between the two waveguides. The same approach was used to determine the mode content in the FDTD simulated fields The steady state fields were multiplied by the unit-basis functions and integrated over the cross section to obtain voltage and current coefficients for each mode. These were then converted to forward and backward travelling waves.

Figure 5 shows a vector plot of the FDTD simulated fields for the step transition. A TE_{11} mode having 1.0 volt amplitude was launched in the small waveguide using equivalent surface currents. The scattering matrix **S** was determined theoretically and the expected transmissions and reflections of the step are given by

$$\mathbf{b} = \mathbf{S}\,\mathbf{a} \tag{3}$$

where **a** and **b** are the sets of modes entering and leaving the junction respectively. Table 1 shows mode voltage coefficients computed from the FDTD output file . Waves travelling in the +z direction in region I and in the -z direction in region II are the inputs, i.e. they form the **a** vector in (6). Except for the TE_{11} source, all of the coefficients in **a** are caused by reflections from the RBC's. Table 2 compares the expected transmission and reflection against the numerical outgoing waves. It also lists the values expected if no boundary reflections had occurred. This shows excellent agreement for the propagating modes in each waveguide.

Note that the boundary reflections were small for the TE_{11} mode, but they were larger for higher-order modes because of the different phase velocities. The TE_{12} mode in region II experienced a 37% reflection. This highlights the need for a true multi-mode RBC. The simulation shown was run on an IBM 3090/600S computer using a 69x69x70 model and required approximately 3100 cpu seconds for 6500 time steps. A time history plot showed steady state conditions after approximately 1200 time steps. The cell size was 1/32nd of the free space wavelength.

VII. Summary

This paper has demonstrated the validity of the Finite-Difference Time Domain method for waveguide scattering analysis, even when modeling higher-order modes in stair-stepped cylinders. Source conditions and absorbing boundary conditions were described which provide good stability and dynamic range for scatter calculations. The effective cylinder size can be determined from its cavity resonance, allowing accurate modeling without excessive spatial resolution. Transmission and reflection coefficients for a waveguide step transition were calculated and showed good agreement with theoretical predictions.

This work was supported by Harry Diamond Laboratories through EG&G, Inc. / Idaho National Engineering Laboratory.

References

[1] P. Alinikula, K. S. Kunz, "Analysis of Waveguide Aperture Coupling Using the Finite-Difference Time-Domain Method," *IEEE Microwave and Guided Wave Letters*, vol.1, no.8, Aug. 1991, pp. 189-191.

[2] M. De Pourcq, C. Eng, "Field and power-density calculations in closed microwave systems by three-dimensional finite differences," *IEE Proceedings*, vol. 132, October 1985, pp. 360-368.

[3] M. F. Iskander, O. Andrade, H. Kimrey, R. Smith, S. Lamoreax, "Computational Techniques in Modeling and Quantifying Microwave Interactions with Materials," *Proceedings of the 93rd American Ceramic Society Meeting*, Apr. 28-May 2, 1991, vol. 12, pp. 141-158.

[4] A. Taflove, K. R. Umashankar, "The Finite-Difference Method for Numerical Modeling of Electromagnetic Wave Interactions with Arbitrary Structures," Chapter 8 in *PIER 2 Finite Element and Finite Difference Methods in Electromagnetic Scattering*, edited by M. A. Morgan, Elsevier, 1990.

[5] R.F. Harrington, *Time-Harmonic Electromagnetic Fields*, McGraw-Hill, New York, 1961.

[6] D. E. Merewether, R. Fisher, F. W. Smith, "On Implementing a Numeric Huygen's Source Scheme in a Finite Difference Program to Illuminate Scattering Bodies," *IEEE Trans.*, vol. NS-27, Dec. 1980, pp. 1829-1833.

[7] G. Mur, "Absorbing Boundary Conditions for the Finite-Difference Approximation of the Time-Domain Electromagnetic-Field Equations," *IEEE Trans.*, vol. EMC-23, May 1981, pp. 377-382.

[8] K. K. Mei, "Time-Domain Finite Difference Approach to the Calculation of the Frequency-Dependent Characteristics of Microstrip Discontinuities," *IEEE Trans.*, vol. MTT-36, no.12, Dec. 1988.

[9] N. Marcuvitz, *Waveguide Handbook*, McGraw-Hill, New York, 1951.

[10] J. M. Baird, D. H. Roper, R. W. Grow, "Surface Array Waveguide Mode Analyzer," this digest. (*IEEE 1992 International Microwave Symposium Digest* MTT-S)

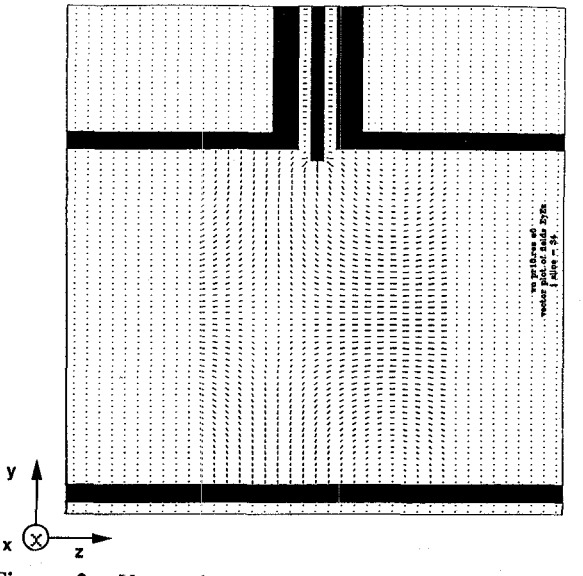

Figure 2 Vector plot of electric fields of the TM_{01} mode in a circular waveguide with a coaxial probe.

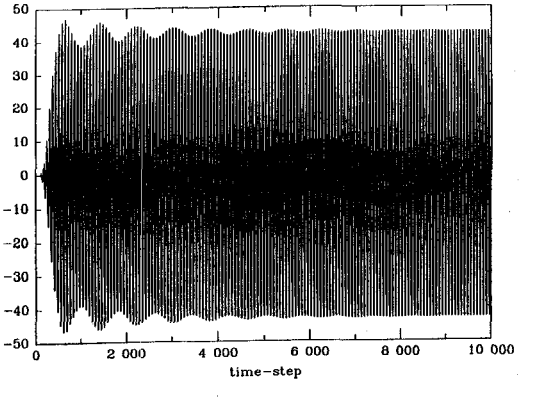

(a)

Figure 3 Time history plots of fields in a uniform waveguide (a) inside and (b) outside the TFZ.

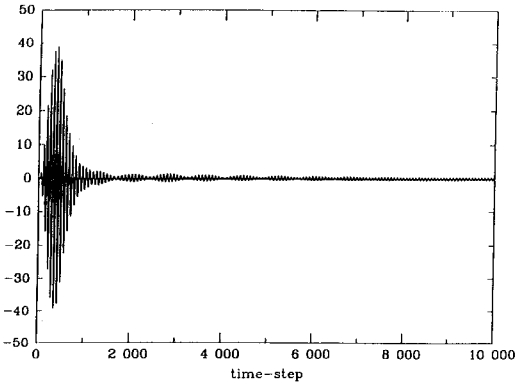

(b)

Figure 3 Time history plots of fields in a uniform waveguide (a) inside and (b) outside the TFZ.

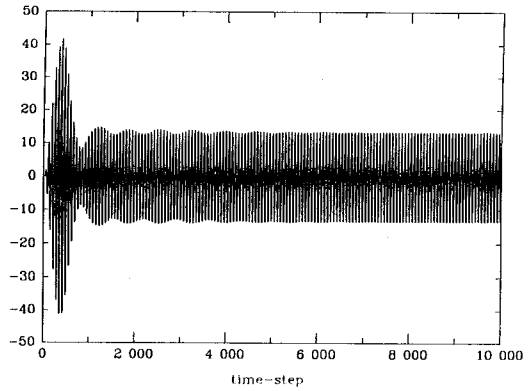

Figure 4 Initial field calculation for a point outside the TFZ. Fields are expected to decay to zero at this position.

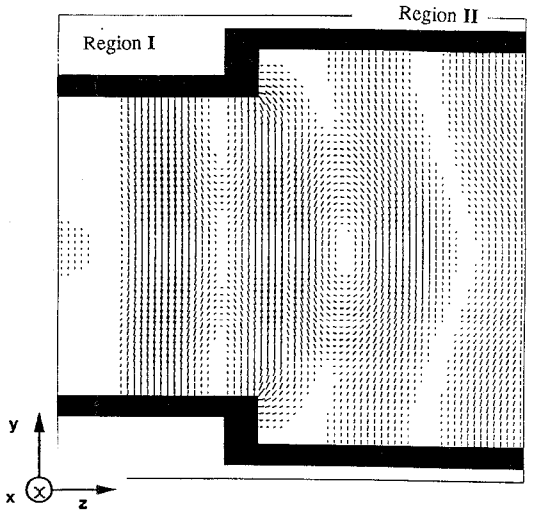

Figure 5 Vector plots of electric fields in circular stepped waveguides (longitudinal direction).

mode	V^+ in wg I	V^- in wg II
TE_{11}	.9931 < 98°	.0029 < -52°
TM_{01}	.0001 < -156°	.0001 < 145°
TE_{21}	.0015 < -175°	.0009 < -171°
TE_{01}	.0014 < 177°	.0006 < -156°
TM_{11}	.0274 < -17°	.0293 < 126°
TE_{31}	.0050 < -112°	.0011 < -156°
TM_{21}	.0002 < -55°	.0002 < -28°
TE_{41}	.0004 < 118°	.0004 < 134°
TE_{12}	.0096 < 120°	.1451 < 80°
TM_{02}	.0001 < -63°	.0001 < -49°

Table 1 Computed voltage coefficients at the reference planes for modes entering the junction.

Reflection

mode	FDTD	Eq. (3)	Single input
TE_{11}	.0596 < 69°	.0600 < 63°	.0691 < 76°
TM_{01}	.0001 < 23°	.0000 < 0°	.0000 < 0°
TE_{21}	.0015 < 5°	.0000 < 0°	.0000 < 0°
TE_{01}	.0014 < -4°	.0000 < 0°	.0000 < 0°
TM_{11}	.1149 < -15°	.1135 < -12°	.1312 < -27°
TE_{31}	.0034 < -26°	.0000 < 0°	.0000 < 0°
TM_{21}	.0002 < 123°	.0000 < 0°	.0000 < 0°
TE_{41}	.0004 < -61°	.0000 < 0°	.0000 < 0°
TE_{12}	.0151 < 22°	.0053 < 13°	.0075 < 155°
TM_{02}	.0001 < 121°	.0000 < 0°	.0000 < 0°

(a)

Transmission

mode	FDTD	Eq. (3)	Single input
TE_{11}	.8710 < -77°	.8694 < -76°	.8864 < -77°
TM_{01}	.0001 < -32°	.0000 < 0°	.0000 < 0°
TE_{21}	.0009 < 9°	.0000 < 0°	.0000 < 0°
TE_{01}	.0006 < 26°	.0000 < 0°	.0000 < 0°
TM_{11}	.2788 < 14°	.2678 < 14°	.2558 < 15°
TE_{31}	.0081 < 103°	.0000 < 0°	.0000 < 0°
TM_{21}	.0002 < 152°	.0000 < 0°	.0000 < 0°
TE_{41}	.0005 < 137°	.0000 < 0°	.0000 < 0°
TE_{12}	.3966 < -67°	.4101 < -56°	.3145 < -40°
TM_{02}	.0001 < 137°	.0000 < 0°	.0000 < 0°

(b)

Table 2 Comparison of computed coefficients and analytic solution: Table 1 inputs and single-mode input. (a) Refl. waveguide I (b) Trans. in waveguide II.